crystals

MDPI

Article

Development of Geopolymer Foams for Multifunctional Applications

Adrienn Boros * and Tamás Korim

Department of Materials Engineering, Faculty of Engineering, University of Pannonia, H-8201 Veszprém, Hungary; ktm042@almos.umi-pannon.hu
* Correspondence: boros.adrienn@mk.uni-pannon.hu; Tel.: +36-88-624-000 (ext. 6067)

Abstract: Due the increasingly stringent environmental regulations and sustainable development-induced pressures to increase efficiency, the world faces new challenges. For this reason, the production of structural materials with controlled properties has become urgent. Due to their excellent mechanical and chemical properties and energy-efficient production methods, geopolymers have remarkable potential in higher value-added applications. This potential application exceeds their historical use as environmentally friendly substitutes for Portland cement. The aim of the present research is to produce metakaolin-based geopolymer foams using the combined technique of saponification/peroxide decomposition/gel casting. Concerning physical properties, the effect of H_2O_2 concentration, the type and amount of stabiliser and the addition of slag were investigated. XRD, FTIR, SEM, CT and thermogravimetric analyses were performed to characterise the material structure. Multifunctional geopolymer foams were developed that can be made free of organic matter and cracks through the optimisation of technological parameters (heat treatment, washing and firing). Such high strength (8.9 MPa), lightweight (~499 kg/m^3) and low thermal conductivity (~0.041 W/mK) foams can be used as thermal insulating materials to reduce the energy loss of buildings. Due to their high open porosity (~77.7 vol%) and specific surface area (~4.3 m^2/g), foamed geopolymers can function as catalyst supports in many physicochemical applications.

Keywords: foamed geopolymer; combined foaming process; controlled physical properties; structural characteristics; multifunctional applications; thermal insulating material; catalyst support; organic matter; crack-free foam

check for updates

Citation: Boros, A.; Korim, T. Development of Geopolymer Foams for Multifunctional Applications. *Crystals* **2022**, *12*, 386. https://doi.org/10.3390/cryst12030386

Academic Editors: Michał Łach, Kinga Korniejenko, Wei-Ting Lin and Neslihan Dogan-Saglamtimur

Received: 19 February 2022
Accepted: 11 March 2022
Published: 13 March 2022

Publisher's Note: MDPI stays neutral with regard to jurisdictional claims in published maps and institutional affiliations.

Copyright: © 2022 by the authors. Licensee MDPI, Basel, Switzerland. This article is an open access article distributed under the terms and conditions of the Creative Commons Attribution (CC BY) license (https://creativecommons.org/licenses/by/4.0/).

1. Introduction

Alkali-activated inorganic polymers (AAIP) or geopolymers (GP) are not only the structural materials of the future but also of the present; they are intensively researched material systems. Early research has shown that GPs can be cheaply produced by way of reacting naturally occurring aluminosilicates with alkali metal silicate/hydroxide solutions [1,2]. The exothermic reaction under strongly alkaline conditions takes place at atmospheric pressure and at a temperature below 100 °C [3]. The mechanism of geopolymerisation shows many similarities to the synthesis of zeolites, although the reaction products that are formed during the two processes have different structures and chemical compositions. GPs are amorphous or semicrystalline three-dimensional polymers; in their sialate network, SiO_4 and AlO_4 tetrahedron units are connected by bridging oxygen atoms. Alkali cations (e.g., Na^+, K^+ and Ca^{2+}) balance the positive charge deficit resulting from the substitution of Si^{4+} and Al^{3+} [4].

For a long time, it was believed that GPs, due to their excellent mechanical and chemical properties, could be realistic alternatives to classic binders, especially to traditional Portland cement (OPC). However, as a result of accumulating knowledge, there is now growing concern that Portland cement-based binders cannot be fully replaced by these new types of inorganic polymers. On the other hand, it is certain that GPs can be serious competitors to classical binders in some areas of the building, automotive and nuclear industries

(e.g., masonry and thermal insulation bricks, pourable road and pavement layers, refractory composites and immobilisation matrices of hazardous and radioactive wastes) [5–11]. With the production of lightweight/foamed structural elements, individual applications may also appear. As eco-friendly porous materials, GP foams have considerable potential in environmentally and economically relevant fields (e.g., air and wastewater treatment) due to their favourable production conditions and promising properties [12–15].

The foaming of GPs can occur in several ways (e.g., direct foaming, replica method, release filler method, additive manufacturing, etc.); out of these, direct foaming is the most common method [16]. The primary production process of GP foams is chemical foaming, which is based on the evolution of gas in viscous slurry. Two types of such processes are known: in a strongly alkaline medium, the component added to the aqueous matrix (a) decomposes thermally (e.g., H_2O_2) or (b) undergoes a chemical reaction (e.g., silica fume, aluminium paste and metal Al or Si). As a result of the released O_2/H_2 gas, the slurry begins to expand, and during the bonding and solidification process, the bubbles formed are trapped, thus creating a typically closed macroporous network [13,15,17–23]. However, it should be noted that wet foams formed with the help of these methods are thermodynamically unstable systems in which—due to the surface tension at the gas–slurry interface—the entrapped bubbles start to coalesce, which can also lead to the collapse of the formed pore structure [12,18,20,22,24,25].

In order to avoid collapse of the pore structure, components are added to the GP slurry to stabilise the interface between the liquid and gas phases through the adsorption of their molecules and the formation of micelles (after reaching a critical micelle concentration). These stabilisers are usually commercially available surfactants (e.g., Pluronic L35, Tween 80, Triton X100, SDS (sodium dodecyl sulphate), sodium oleate, Sika® AER5 and CTAB (cetyltrimethylammonium bromide) [16,24,26–28]) or triglycerides (animal and vegetable fats, oils and proteins). From the latter, surfactant is formed in situ during the saponification reaction in an alkaline environment [16,25,29–31]. Through the joint use of chemical blowing agents and surfactants, the macroporous network, i.e., the relative proportions of closed and open pores, can be managed as desired [16,24,25,27–32]. Cilla et al. [29] were able to produce GP foams with a pore content of up to 85 vol% (with 70 vol% open porosity) using a combination of different vegetable and animal fatty acids and H_2O_2. However, when using this combined SPG (saponification/peroxide decomposition/gel casting) technique, the compressive strength of the foams will be only 0.2–0.4 MPa, which limits their field of application.

For practical application, it is essential not only to control the pore size and distribution but also to ensure the optimum strength with high interconnected porosity; the contrast between the latter two features is easily noticeable. The type, shape, size and distribution of the pores have significant influence on the physical properties of the resulting foams. While round and homogeneously distributed pores improve the thermal insulating properties of foams, irregularly shaped and heterogeneously distributed cavities form a complex network whose interconnected air ducts improve the acoustic resistance [12,16–18,20]. Commercially available organic insulators (e.g., polystyrene (EPS and XPS) and polyurethane) used for such purposes are flammable, and the production of their inorganic counterparts (e.g., foamed glass, expanded perlite and mineral wool) is extremely expensive [21–23]. In contrast, GP foams are non-flammable, do not require complex technology to produce and have a thermal conductivity comparable to that of the most commonly used insulating materials [12,17,21–23].

Much of the literature deals with applications for the construction industry [5–11,17,18,20–23,27]; still, an increase in the efficiency necessary for sustainable development enhances several environmental problems that can be mitigated using GP foams. The purification of air and wastewater can be accomplished through photocatalytic reactions in which the formation of the catalyst supports plays a major role. In addition to a controlled pore structure and a high specific surface area, chemical inertness, high permeability, adequate mechanical strength, stability and surface finish are also essential requirements [12,14–16,33]. Transition

metal ions can be incorporated into the network of hierarchically porous foams (as in the case of zeolites), which can act as active centres for catalytic reactions [13,15,34], thus providing viable solutions for reducing the organic matter contents of the atmosphere and wastewater [12,14,16,33,35].

The present study investigates metakaolin-based GP foams produced with the help of the SPG combined technique and extends to the exploration of the relationship between the physical properties and material structure characteristics. Due to the previously stated sustainable development-induced pressures to increase the efficiency and the obvious benefits of geopolymer foams, the aim of this research is to develop a manufacturing process that allows the produce of multifunctional foams. In the scope of this study, experiments to produce organic matter and a crack-free sample with high strength and high open porosity were performed, based on which, the foamed geopolymer can be deemed a promising insulating material, as well as a catalyst support.

2. Materials and Methods

2.1. Materials

The metakaolin (MK) used as the raw material for the experiments was obtained by calcining New Zealand kaolin at 750 °C for 8 h. The mineral composition of MK (Table 1) was determined with the help of X-ray diffraction (XRD). MK contains a large amount of the amorphous phase (92.4 wt%); additionally, quartz and cristobalite are present as crystalline phases (see Figure A1 in Appendix A). The chemical composition of calcined kaolin (Table 2) was determined with the help of X-ray fluorescence spectrometry (XRFS). The particle size distribution of MK and its median (D50) were determined with the help of a laser granulometer, 14.7% < 2 μm, D50 = 23.93 μm (see Figure A2 in Appendix A).

Table 1. Phase compositions of metakaolin (MK) and slag (GGBFS).

	Quartz	Cristobalite	Merwinite	Akermanite	Brownmillerite	Vitreous Phase
MK	4.6	3	-	-	-	92.4
GGBFS	0.2	-	11.1	1.2	0.6	86.9

Table 2. Chemical compositions (wt%) of metakaolin (MK) and slag (GGBFS).

	SiO_2	Al_2O_3	TiO_2	Fe_2O_3	CaO	MgO	Na_2O	K_2O	SO_3	LOI
MK	56.26	38.04	0.17	0.88	0.54	0.47	0.42	0.95	-	2.16
GGBFS	34.05	6.45	-	-	47.36	8.06	1.08	0.57	1.48	0.95

Analytical-grade sodium-hydroxide pellets (Reanal Laborvegyszer Kereskedelmi Kft., Budapest, Hungary) and sodium silicate solution (ANDA Kft., Barcs, Hungary, with the chemical composition 28.6 wt% SiO_2, 6.8 wt% Na_2O and 64.6 wt% H_2O) were used as the activating solution. During the foaming process, sodium oleate (Sigma-Aldrich Chemie GmbH, Steinheim, Germany) and two vegetable oils (olive oil (Aceites Borges Pont, SAU, Tàrrega, Spain) and sunflower oil (NT Kft., Kiskunfélegyháza, Hungary)) were used as stabilising agents. The foaming agent was prepared by way of diluting a 30 wt% H_2O_2 solution (Reanal Laborvegyszer Kereskedelmi Kft., Budapest, Hungary).

For the purpose of reducing the shrinkage tendency of foams—based on the results by Samson et al. [36]—MK was partially replaced by ground-granulated blast furnace slag (GGBFS) provided by ISD DUNAFERR Zrt. (Dunaújváros, Hungary). Based on the XRD recording (see Figure A3 in Appendix A), it can be established that GGBFS contains 86.9 wt% amorphous phase, with merwinite as the main crystalline phase, and—in addition—akermanite, bronwmillerite and quartz are also present as minor components (Table 1). The chemical composition of GGBFS is shown in Table 2. The slag has a heterogeneous particle size distribution, and it contains an amount of 13.4% particles smaller than 2 μm, D50 = 13.84 μm (see Figure A4 in Appendix A).

2.2. Sample Preparation

Solid NaOH was dissolved in water glass for the preparation of the activating solution (AS). The sodium silicate modulus (SiO_2/Na_2O) of the AS was 1.2, and the amount of Na_2O with respect to the dry metakaolin mass was 29.4 wt%. During the experiments, the following molar ratios were used to prepare the GPs: SiO_2/Al_2O_3 = 3.5 and Na_2O/Al_2O_3 = 1.3. First, the AS was cooled to the appropriate temperature, and the required amount of MK was added. During the mixing, identical conditions were ensured, i.e., the slurry of the starting material-alkaline solution was mixed mechanically for 5 min at 900 rpm. Second, various stabilising agents were added to the slurry, and the resulting mixture was further homogenised for 5 min at 1200 rpm. Finally, the H_2O_2 solution was added the obtained mixture, which was mixed for 1 min at 600 rpm.

The prepared fresh mixture was cast into sealed 35 × 35-mm cylindrical PVC moulds, then cured for 24 h at ambient conditions (T = 21–23 °C and RH = 50 ± 10%) and then for another 24 h at 75 °C (based on research settings by Bai et al. [30]) before demoulding. The hardened foams were demoulded at 2 days of age, and the tests were performed at 7 days of age.

In the first stage, the amounts of stabiliser (S) and foaming agent (F) (S = 0.2 × (MK + AS), F = 0.1 × (MK + AS)) were fixed, and varied concentrations of H_2O_2 solution were applied: 0, 3, 6, 9, 12, 15, 18, 21, 24, 27 and 30 wt% solutions diluted from 30 wt% H_2O_2. Intermediate concentrations (4.5 and 7.5 wt%) were also used, taking into account the relevant physical properties.

In the second stage, GP foams prepared with sunflower oil and 4.5 wt% H_2O_2 solution (S:F = 2.0:1.0) were selected as the optimums (based on the results of the previous stage). For removing excess organic matter content, the foams were washed in continuous operation (at 80 °C for 1 h), dried at 40 °C for 1 week and then heat-treated at 600 °C. The material structure characteristics of the samples were investigated before washing (bw), after washing (aw) and after firing (af). The bonding conditions (FTIR), the phase composition (XRD) and the morphological properties (SEM) of the formed polymer structure were determined. The organic matter content of the foams was monitored by way of a CHNS elemental analysis.

During the experiments, several problems occurred: oil precipitation on the surface of already hardened specimens, entrapped soap and glycerol molecules within the pores, surface hairline cracks and internal microcracks. In the third stage, our goal was to solve the above-mentioned problems. With a fixed H_2O_2 content, the S:F ratio (2.0:1.0, 1.5:1.0, 1:1.0, 0.5:1.0, 0.25:1.0, 0.1:1.0 and 0.05:1.0) was altered in order to minimise the oil content. In order to remove the soap and glycerol molecules from the pores, the washing parameters were modified. The originally applied continuous washing was changed to intermittent operation (at 80 °C, with water replacement every half-hour). For reducing the shrinkage tendency, the MK was partially replaced by GGBFS (10–50 wt%). In order to eliminate the cracks, the storage conditions were changed: room temperature, laboratory atmosphere (T = 21–23 °C and RH = 50 ± 10%) and underwater storage (T = 21–23 °C) were applied. For preventing an abrupt loss of water from the samples due to heat treatment, the open/closed (OM/SM) state of the moulds and the initial heat treatment parameters were changed:

1. 24 h at 21–23 °C and another 24 h at 75 °C in SM,
2. 24 h at 40 °C in SM,
3. 24 h at 60 °C in SM,
4. 24 h at 60 °C in OM,
5. 1 h at 80 °C in SM and another 4 h at 80 °C in OM.

2.3. Methods

The particle size distribution of MK and GGBFS and their median (D50) were determined with the help of Fritsch Laser Particle Sizer "Analysette 22". In order to achieve proper dispersion and to eliminate the intergranular aggregation prior to the start of the

tests, the samples were treated in a water bath equipped with an ultrasonic stirrer and pump for 60 s.

The XRD analyses of the starting materials and the prepared GP foams were carried out using a Philips PW 3710 X-ray diffractometer. The parameters applied were as follows: CuKα radiation (50 kV, 40 mA), 0.02° 2Θ/s speed (in the 2Θ range, 10–70°) and graphite monochromator. The device control and data collection were performed using an X'Pert Data Collector. To evaluate the X-ray diffractograms and to carry out a Rietveld analysis, X'Pert Highscore Plus software and the ICDD PDF-2 reference database were used.

The compressive strength of the foams at the age of 7 days was determined with the help of a CONTROLS Automax5 device using a load force of 2400 N/s, in line with the relevant cement standard (EN 196-1). However, the size of the samples (ø35 $\times$ 35-mm cylinders) differed from the standard. Prior to the start of the test, the surfaces of all specimens were ground flat and parallel. Three parallel measurements were performed with respect to each mixture, and the average values were reported.

The bulk density and apparent porosity of the produced GP foams were determined through the Archimedes method. The samples were placed in distilled water and boiled for 2 h. The specimens were then cooled, and their water-saturated weight was measured in air and through immersion in water with the use a hydrostatic balance.

The thermal conductivity of the foams was determined according to the ASTM-D7984 standard using a modified transient plane source method (MTPS) with the help of a C-Therm TCi device (measuring range: 0.002–220 W/mK). Prior to the start of the tests, the surfaces of the samples were ground flat, and the dust in the exposed pores was removed.

For the determination of the optimal firing temperature of the samples, a thermogravimetric (TG) analysis was performed. During the measurement, 300 mg of sample was examined. The TG curve was recorded with the help of a Q 1500D derivatograph using a heating rate of 10 °C/min, air atmosphere and a corundum reference. The measurement was performed in the range of 20–1000 °C.

Morphological studies of GP foams were performed with the help of an FEI/ThermoFisher Apreo S scanning electron microscope (low vacuum mode) and a computer-controlled imaging system with an accelerating voltage of 20 kV for backscattered (BSE) and 10 kV for secondary electron (SE) imaging. The elemental compositions of the samples were determined using an EDAX AMETEK Octane Elect plus energy dispersive X-ray analyser. The accelerating voltage was 20 kV, and the data collection time was 180 s.

The pore size distribution of the foams was determined using a Keyence VHX-2000 digital light microscope. Before the examination, the cross-sections of the samples were ground flat. The pore size distributions were obtained through taking the average of 100 pore diameters.

FTIR analyses of GP foams were carried out with the help of a Perkin Elmer Spectrum Two device equipped with a platinum ATR adapter. The reflectance spectrum was recorded by averaging 512 spectra during the measurements.

The organic matter contents of the samples were monitored using a Carlo-Erba EA 1108 CHNS-O elemental analyser. The technique used for the determination of organic matter contents is based on the quantitative "dynamic arc burning" method. During the measurements, tin capsules, a 1020 °C combustion reactor and a stream of helium enriched in pure oxygen were used. The resulting gases were separated on a packed gas chromatography column and quantified with the help of a thermal conductivity detector (TCD) (measuring time: 7 min, range: 100 ppm-100%).

Computed tomography (CT) images of GP foams were prepared using a Nikon XT H 225 ST X-ray tomography and associated VG Studio 3.4 software. The following parameters were used during the measurements: an accelerating voltage of 160 kV, a cathode current of 85 µA, 1250 projection/recording, 2 recordings per projection and a 500-ms data collection time.

The specific surface area values of the foams were determined with the help of the application of the single-point Brunauer–Emmett–Teller (BET) method using a MICROMERITICS Flowsorb II 2300 type instrument.

3. Results and Discussion

3.1. The Physical Properties of MK-Based GP Foams

In the first stage of the experiments, MK-based GP foams were prepared using a fixed stabiliser:blowing agent ratio (S:F = 2.0:1.0) and a varied concentration of the H_2O_2 solution (3–30 wt%). "Dense" samples (0 wt% H_2O_2) were also prepared as references, where the required amount of H_2O_2 solution was replaced by distilled water to maintain the S:F = 2:1 ratio. Irrespective of whether the foams are structural materials with thermal insulation properties or catalyst supports, the products must have appropriate strength. As the minimum strength grade of building blocks made from aerated concrete must reach a compressive strength of 1.0 MPa (according to the GB11968-2006 standard), this value was considered authoritative in this study. It is important to note that the aim of the present research is to develop a foam with high open porosity (>50 vol%) and adequate strength (>1 MPa) using different foam precursors (olive oil (O), sunflower oil (S) and sodium oleate (SO)) and H_2O_2. The purpose of the comparative study with three soap precursors was to select the type of stabiliser and the concentration of H_2O_2 solution that can be used to produce foam that meets the mentioned requirements. Figure 1 shows the obtained compressive strength and porosity values, and Table 3 summarises the results obtained during the determination of thermal conductivity. By way of increasing the concentration of the foaming agent, the porosity and pore size distribution of the samples could be altered.

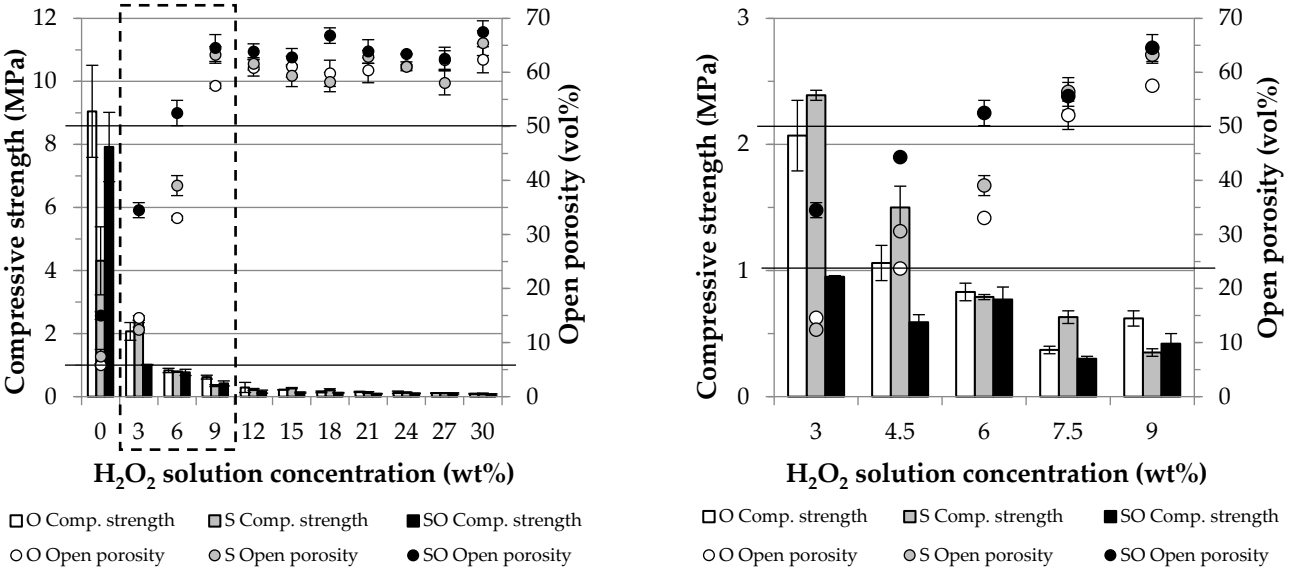


Figure 1. Effect of the H_2O_2 solution concentration in the range of (**a**) 0–30 wt% and (**b**) 3–9 wt% on the compressive strength and open porosity of GP foams using different stabilising agents (Horizontal lines indicate boundary conditions in the case of the experimental job).

Table 3. Effect of H_2O_2 solution concentrations on the thermal conductivity of GP foams when using different surfactants.

H_2O_2 Solution Concentration (wt%)	Heat Conductivity (W/mK)		
	Olive Oil	Sunflower Oil	Sodium Oleate
0	0.110 ± 0.024	0.103 ± 0.027	0.073 ± 0.005
3	0.068 ± 0.010	0.099 ± 0.009	0.056 ± 0.006
4.5	0.052 ± 0.002	0.056 ± 0.007	0.048 ± 0.005
6	0.049 ± 0.002	0.051 ± 0.003	0.051 ± 0.002
7.5	0.042 ± 0.002	0.045 ± 0.003	0.045 ± 0.001
9	0.041 ± 0.001	0.041 ± 0.005	0.043 ± 0.004
12	0.042 ± 0.001	0.039 ± 0.001	0.042 ± 0.003
15	0.041 ± 0.002	0.040 ± 0.001	0.044 ± 0.005
18	0.037 ± 0.001	0.036 ± 0.001	0.037 ± 0.001
21	0.038 ± 0.001	0.038 ± 0.002	0.039 ± 0.002
24	0.037 ± 0.003	0.035 ± 0.001	0.037 ± 0.002
27	0.037 ± 0.001	0.034 ± 0.001	0.037 ± 0.001
30	0.035 ± 0.002	0.034 ± 0.001	0.035 ± 0.001

Based on Figure 1, it can be concluded that the curves of the foams produced with different stabilising agents are very similar. The differences in the absolute values of the foams produced with the given H_2O_2 concentrations are caused by the different compositions of the foam precursors. Although both olive oil and sunflower oil are sources of vegetable fatty acids, while olive oil is rich in monounsaturated chains, sunflower oil is rich in polyunsaturated chains. Sodium oleate is the sodium salt of oleic acid, a monounsaturated fatty acid. It is clear that the nature of the fatty acids used greatly influences the surfactant and foaming properties of the soap precursors, which ultimately determine the physical properties of GP foams.

An increase in the concentration of the H_2O_2 solution causes the strength of the foams to decrease monotonically and their porosity to increase monotonically (Figure 1a). It is not preferable to increase the concentration of the foaming agent above a certain value; the relevant changes are observable at low concentrations (3–9 wt%) (Figure 1b). In order to optimise the strength–porosity relationship, intermediate measurement points were used at the 4.5 and 7.5 wt% concentrations, respectively. In line with the findings of the previous results reported in the literature [21,30], it can be stated that the dilution of the H_2O_2 solution favours synthesis, and a more homogeneous pore size distribution with fewer anisotropic pores can be achieved (Figure 2). However, in this stage of the experiments, no foam was capable of meeting both of the requirements ($\sigma_{compressive} > 1$ MPa and $P_{open} > 50$ vol%).

Based on the results reported in Table 3, it can be stated that, similar to the strength and porosity results, there are also more significant changes in the thermal conductivity at low H_2O_2 concentrations. At concentrations of 7.5 wt% and above, foams with extremely good thermal insulation properties and with a thermal conductivity in the range of 0.045–0.034 W/mK can be produced. In the scope of the experiments, an important consideration in selecting the optimal composition was that the produced foams should have the highest possible porosity and should meet the strength-related requirements. Based on the measurement results of their experiments, Bai et al. [30] found that, by way of using olive oil as a stabilising agent, the samples have more favourable physical properties than their counterparts produced using sunflower oil. In contrast, the opposite of this was found in this study; samples made with sunflower oil achieved the best results in terms of the strength–porosity relationship. Differences between the results reported in the given reference and in the present study may also be due to differences in the activator solution composition, oil quality and mixing parameters. A deeper interpretation of the phenomenon requires further experiments.

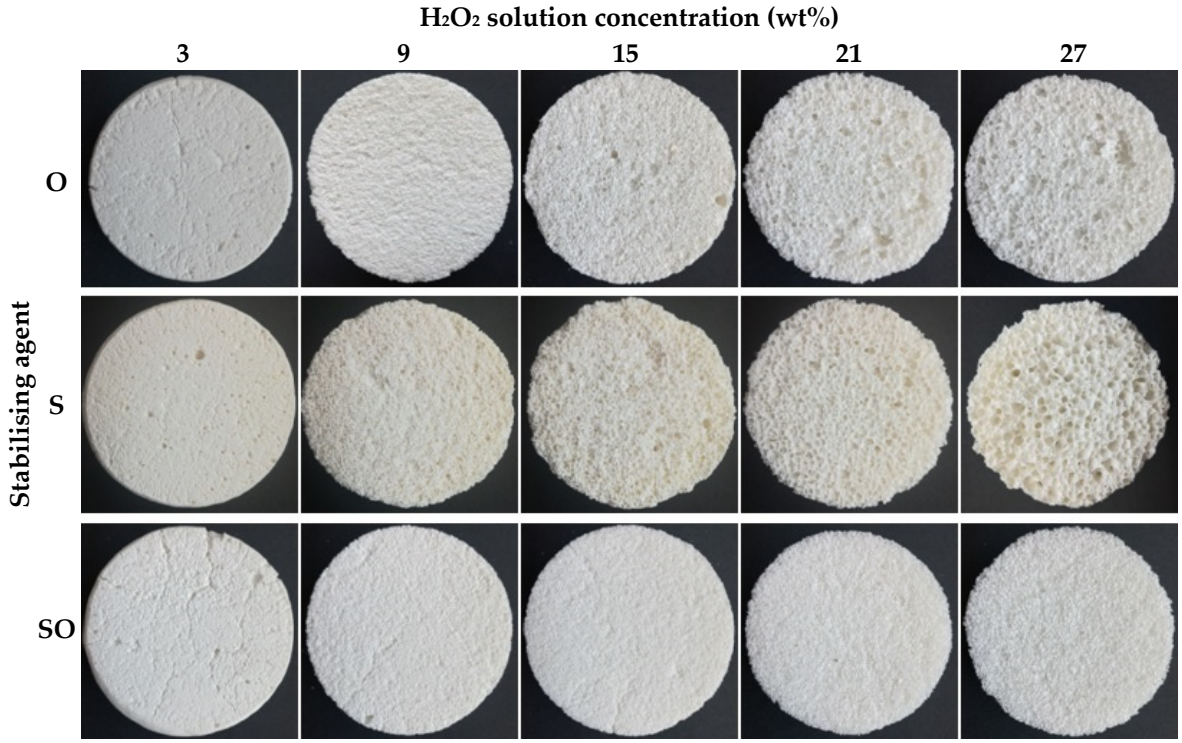


Figure 2. Effect of the dilution of the H_2O_2 solution and type of stabiliser on the pore size.

Foams produced using a foaming agent of 4.5 wt% concentration have adequate strength (1.5 MPa) and can act as catalyst supports due to their sufficiently high open porosity (30.6 vol%). In addition, these foams are structural materials with good thermal insulation properties concerning their thermal conductivity (0.056 W/mK). For these reasons, this composition was used to investigate the relationship between physical properties and structural characteristics. Hereinafter, in the scope of this study, this sample will be referred to as S-4.5.

3.2. The Structural Characteristics of the Optimal Composition

In the second stage of the experiments, in addition to exploring the relationship between the physical properties and material structure characteristics of S-4.5 foam, the aim was to improve the strength, porosity and thermal conductivity results obtained so far. The use of the combined SPG foaming process led to the formation of connected, open pores. During the saponification reaction, water-soluble soap and glycerol molecules were formed in situ, which were present in the structure. This excessive organic matter content yields a problem in terms of later use (whether the material is used as either a thermal insulator or a catalyst support) and should be removed from the foams. For removal, a hot water washing process can be an effective method, which—in addition to extracting the water-soluble components—also makes it possible to check the completion of the geopolymerisation reaction (the incompletely condensed GP structure is sensitive and disaggregates in water). The foams were washed in continuous operation at 80 °C. After 1 h, the water was clear, and no soap foaming was observed; therefore, the procedure was considered successful. Then, the samples were dried at 40 °C for 1 week, and after this, the organic matter content was monitored by way of CHNS elemental analysis (Table 4). Based on the results, it can be established that, even though the water was clear after the 1-h cycle, significant amounts of soap and glycerol molecules were still present in the structure (organic carbon content after washing was 19.1 wt%). Following this, the removal of the organic matter content was to be accomplished by way of firing the S-4.5 sample.

Table 4. Organic matter content of unwashed, washed and fired samples of S-4.5.

Time of Analysis	Amount of Element (wt%)	
	Carbon	Hydrogen
Before washing	23.7	4.1
After washing	19.1	3.6
After firing	5.2	0.5

In order to determine the peak firing temperature, a thermogravimetric analysis was performed; this showed that the organic matter content of the foam completely disappeared when it was heated up to 600 °C (see Figure A5 in Appendix A). The heating rate and holding time not only affected the amount of organic carbon but also critically influenced the shrinkage and crack tendency of the samples; thus, the following gentle firing programme was selected: 30 °C/h heating rate up to 250 °C with 1-h holding time, then 50 °C/h heating rate up to 600 °C and 2-h holding time. Heat treatment at elevated temperatures further reduced the organic carbon content of the foams, but the carbon content did not completely burn out (5.2 wt%). For later use (either as a thermal insulation element or as a catalyst support), this lower organic content can still be a problem and should be removed from the samples. The optimisation of the experimental parameters may function as a good solution to this issue.

The material structure characteristics of the foams (XRD, FTIR and SEM) were determined before washing (bw), after washing (aw) and after firing (af). Regarding mineral composition (Figure 3), it can be said that the main crystalline phase is quartz, and smaller amounts of cristobalite and zeolite are also present. In the range of 18–32° 2θ, amorphous rings were formed, which indicated the organic matter and CASH gel content, the intensity of which decreases during both the washing and the firing processes. This indicated a decrease in the organic matter content.

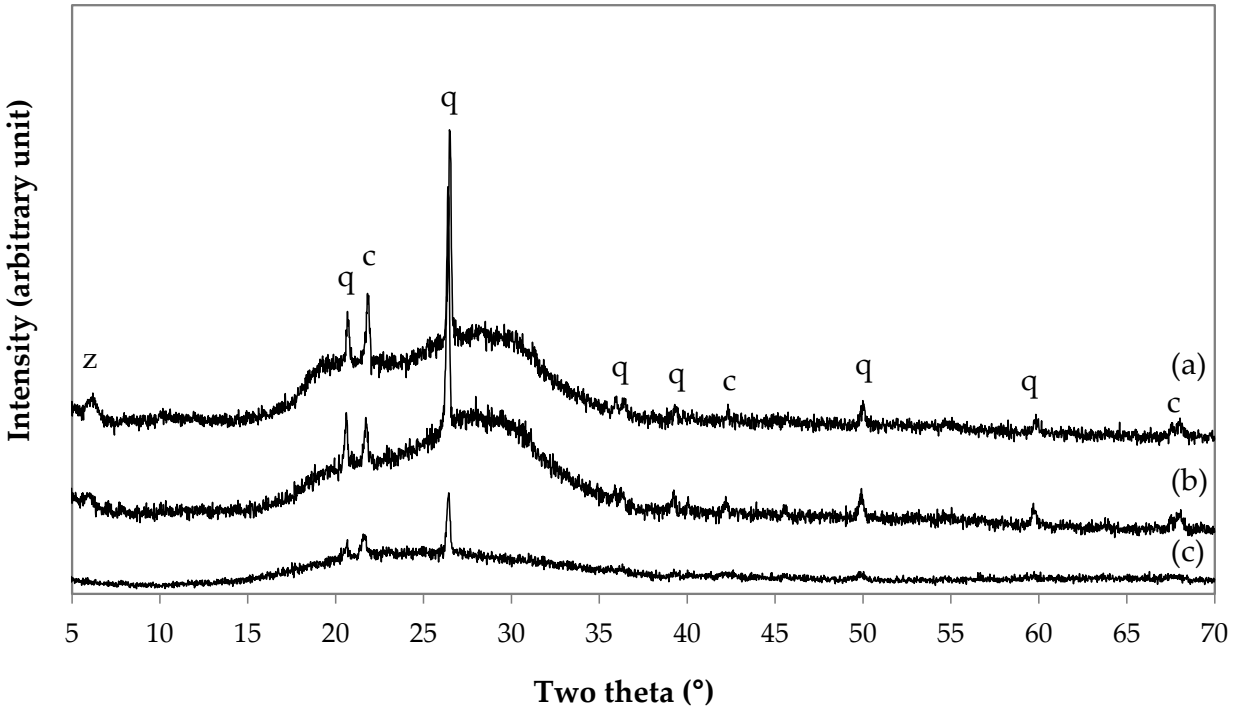


Figure 3. XRD patterns of sample S-4.5 (a) before washing, (b) after washing and (c) after firing (q: quartz PDF 33-1161, c: cristobalite PDF 39-1425 and z: zeolite PDF 01-076-6494).

Evidence for the presence of the organic phase can also be found in the FTIR spectra of the samples (Figure 4): ~3010 (stretching of the C–H– groups), ~2950 (asymmetric

stretching of the –CH_3 groups), ~2920 and 2850 (symmetric and asymmetric stretching of the –CH_2– groups), ~1650 (stretching of –C=C), ~1560 and 1460 (antisymmetric stretching and bending of the –COO– groups) and bands around ~720 cm^{-1} (–CH=CH– bending out of the plane) [37]. The main fingerprint band of the GPs also appears on the spectra: bands around 970–1090 cm^{-1}. After washing, but mainly after firing, there were fewer bands, which is characteristic of the presence of soap and glycerol molecules, and this is in line with the results of the CHNS elemental analysis and XRD analysis.

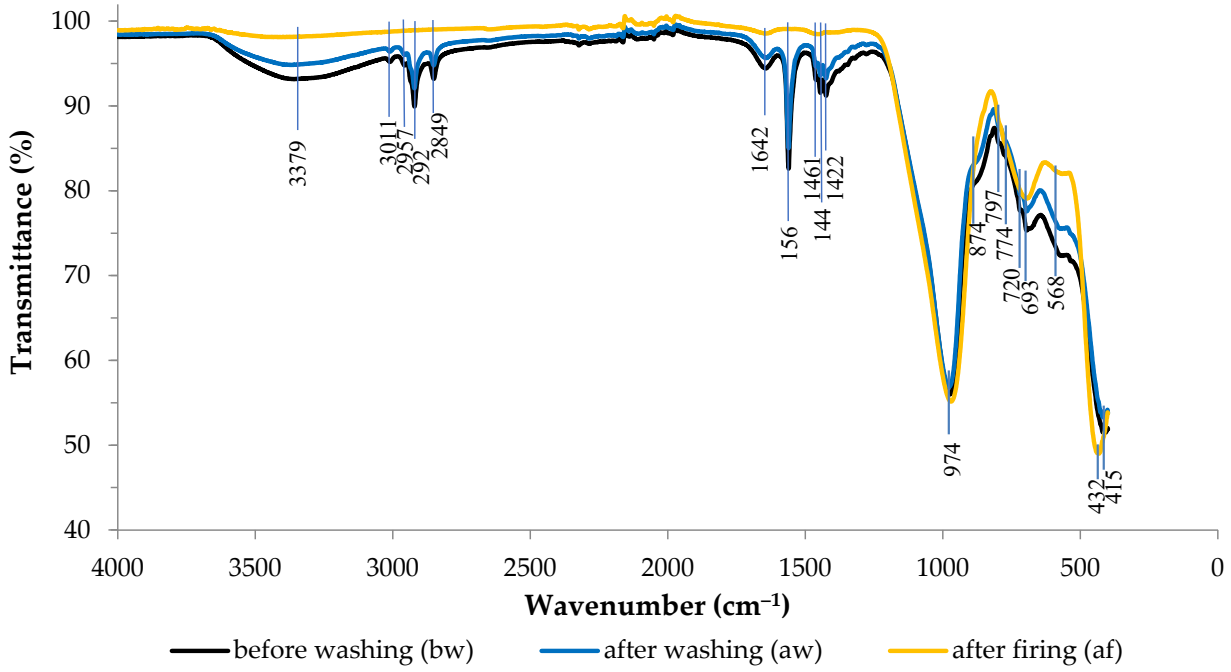


Figure 4. FTIR spectra of unwashed, washed and fired samples of S-4.5.

Regarding the morphology of the samples (Figure 5), it can be said that no significant changes in the microstructure were observed after washing or firing (the average pore size of the samples was 377 ± 140 µm before firing and 367 ± 134 µm after firing).

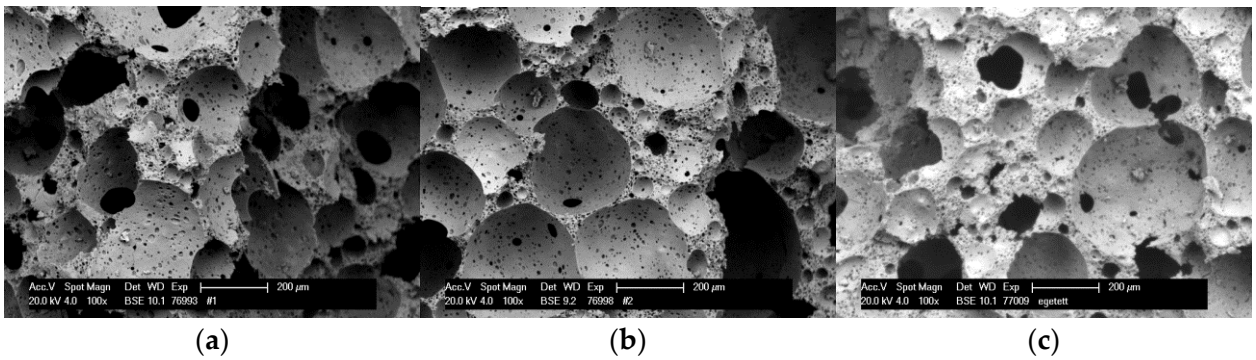


Figure 5. SEM micrograph of (**a**) unwashed, (**b**) washed and (**c**) fired samples of S-4.5.

3.3. The Production of Organic Matter and Crack-Free Foams

As mentioned earlier, several problems occurred in the experiments (Figure 6): the most severe were the organic matter content of the samples, as well as their intense shrinkage and crack tendencies. These problems must be resolved before foams are used as thermal insulation elements or catalyst supports.

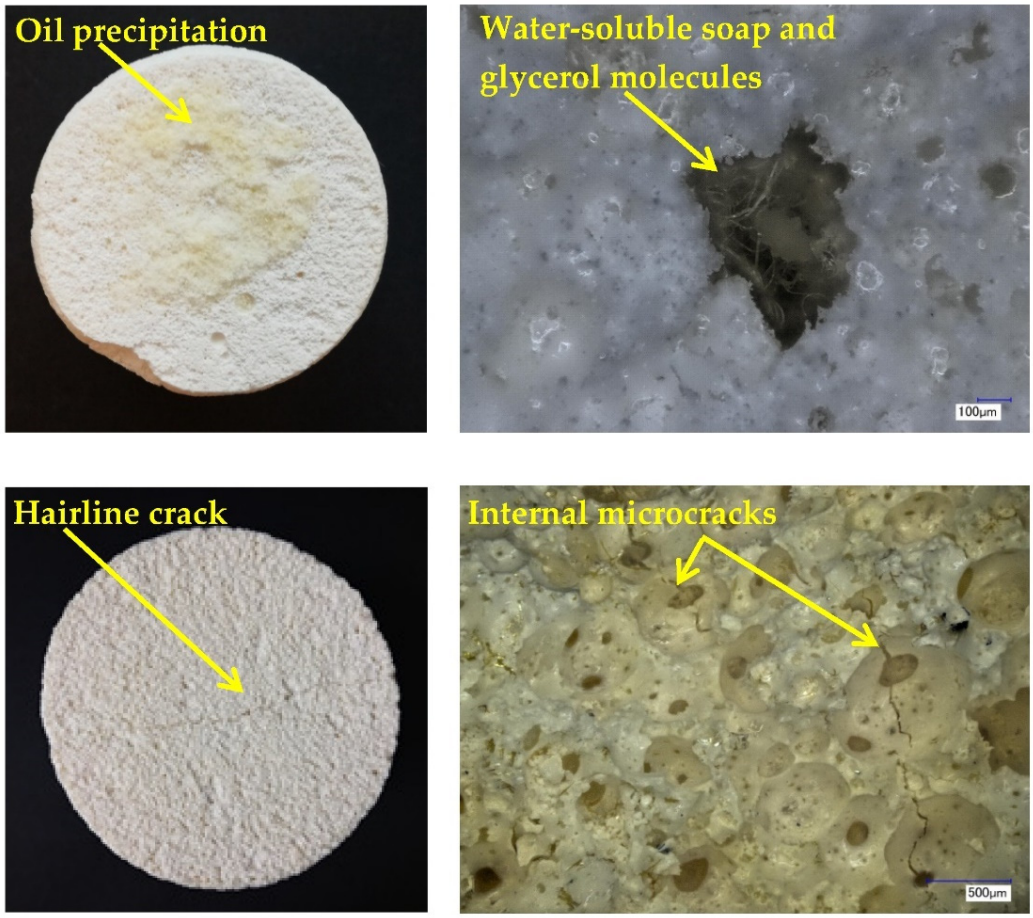
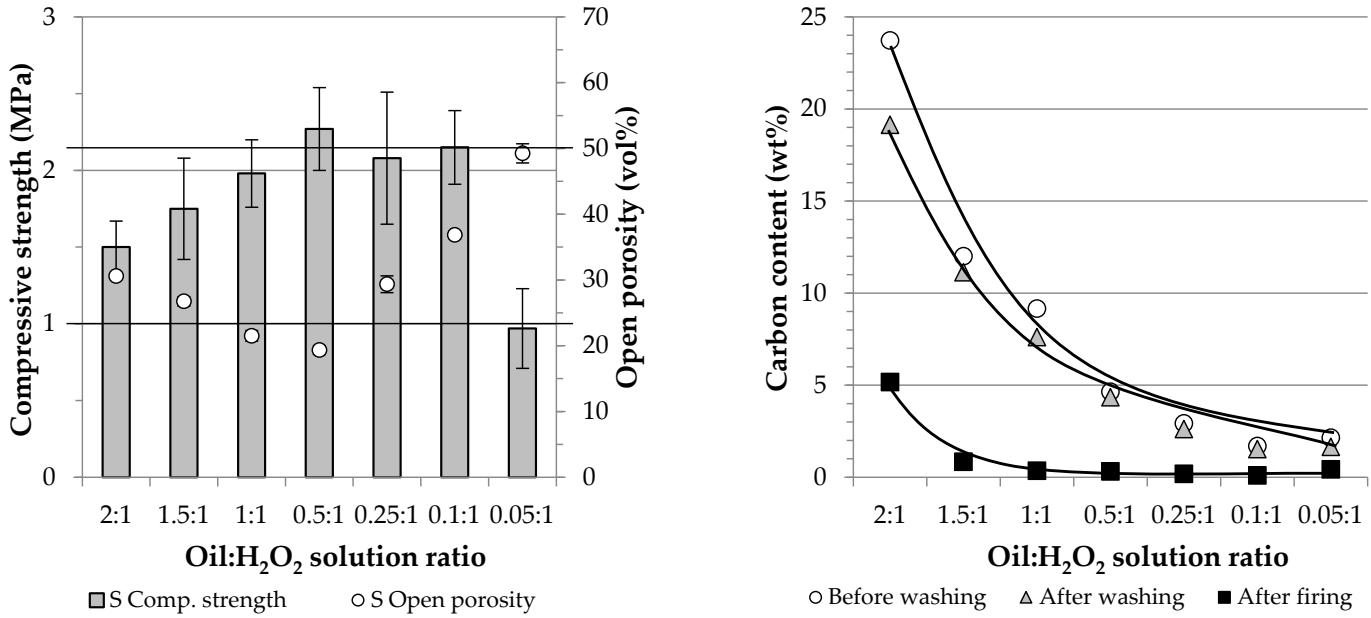


Figure 6. Problems observed during experiments.

3.3.1. The Reduction of the Oil Content

The efficiency of organic matter removal by washing can be increased by reducing the oil content. After drying, the samples made with high S:F ratios (2.0:1.0, 1.5:1.0 and 1.0:1.0) still showed hairline cracks, and the excess oil appeared on their surfaces. However, in the case of the low oil content samples (0.5:1.0, 0.25:1.0, 0.1:1.0 and 0.05:1.0 S:F ratios), the latter problem no longer arose. This suggests that the total amount of triglycerides was converted to surfactants during the saponification reaction. The production of GP foams through the use of the SPG combined technique has been examined in a number of studies [16,25,29,30,32]. There are, however, only a few papers that have demonstrated the effect of the amount of oil content on the physical properties. Bai et al. [30,32] addressed this topic more thoroughly through the saponification of olive oil. They found that an increase in the oil content [30] (from 20 to 70 wt%) decreased the average pore size. This is due to the increasing amount of surfactant formed in the strongly alkaline medium, which facilitated the stabilisation of the gas bubbles. In addition, excess oil droplets that formed during mixing coalesced, thereby increasing the sizes of the interconnecting pores in cell walls and thus reducing the strength of the samples. However, the reduction of the oil content [32] (between 15.00 and 1.25 wt%) did not cause any significant changes in the pore structure, porosity and compressive strength of the samples, which indicates that, up to a certain oil concentration, the effect of the saponification reaction is negligible. Contrary to the authors' experience, in the scope of this study, the reduction of the oil content in the S-4.5 sample (from 20.0 to 0.5 wt%) heavily impacted the physical properties of the foams. The S:F ratio up to a limit of 0.1:1.0 (1 wt% sunflower oil content) had a positive impact but, below this ratio, had a negative effect on the strength (Figure 7a). This was because the amount of surfactant formed in situ was not sufficient to stabilise the gas bubbles that evolved during the decomposition of H_2O_2, which led to pore growth and pore coalescence,

thereby reducing the load-bearing capacity of the samples (in the case of a 0.1:1 ratio, the average pore size was 180 ± 64 μm, while, in the case of the 0.05:1 ratio, the same value was 259 ± 60 μm).



(**a**) (**b**)

Figure 7. Effect of the oil content (**a**) on the compressive strength and open porosity, as well as (**b**) on the organic carbon content (Horizontal lines indicate boundary conditions in the case of the experimental job).

If the oil content was reduced to 1/40 of the initial amount (0.05:1 mixture), the apparent porosity was close to 50 vol%. Even so, in this case, the strength did not meet the 1-MPa requirement. The organic matter content of the samples can be significantly reduced (Figure 7b); while, in the case of the 2.0:1.0 oil:H_2O_2 ratio, the organic carbon content was 23.7 wt%, in the case of the 0.05:1.0 ratio, it was only 2.2 wt%. With respect to these ratios, the organic carbon content of the samples changed from 5.2 wt% to 0.4 wt% after firing.

Based on the relevant physical properties, a mixture with an oil:peroxide ratio of 0.1:1.0 can be deemed the optimum composition: $\sigma_{compressive}$ = 2.2 MPa, P_{open} = 36.9 vol% and λ = 0.052 W/mK. Hereinafter, in the scope of this study, this sample will be referred to as S-4.5-0.1. Through the use of this composition, a ~40% increase in strength and a ~20% increase in porosity over the initial 2.0:1.0 S:F ratio can be achieved. A further advantage of reduction of the oil content was the formation of a more homogeneous pore size distribution (in the case of the 2.0:1.0 ratio, the average pore diameter was 377 ± 140 μm, and in the case of the 0.1:1.0 ratio, it was 180 ± 64 μm).

3.3.2. The Effect of Washing the Parameters

In order to remove the soap and glycerol molecules that formed in situ, the foams were washed; this could be accomplished by both continuous and intermittent operations. The advantage of the former approach was the short washing time (after 1 h, the water was already clear), but its efficiency was debatable, as the organic carbon content of the samples could be reduced only by 10%. In the case of intermittent operation, the reduction of the organic matter content was more significant (25%), but the disadvantage of this method was the long cycle time (the washing water had to be replaced every half hour, and the total washing time was more than 5 h). In this case, at the end of the washing cycle, the water showed a neutral pH, which could indicate that the pore structure of the samples consisted of open, interconnected pores, thereby allowing the free flow of water-soluble

components. However, contrary to the literature [16,29,30], the organic matter content of the foams produced in this study could not be removed completely from the structure through washing (the organic carbon content was 1.3 wt%). It is important to note that, even in this case, the washing stage cannot be omitted. The fact of whether or not the samples were prewashed plays a crucial role in firing. The samples that were not subjected to the washing process got extremely deformed by the firing, and in some cases, they even broke into pieces, while, in the case of the washed samples, neither was this observed (Figure 8).



(**a**) (**b**)

Figure 8. (**a**) Unwashed and (**b**) washed samples after firing. (The left side of the subfigures shows the given sample from a side view, and the right side shows a top view of the same sample.)

3.3.3. The Effect of Slag Addition

Foamed binders are able to exhibit much higher drying shrinkage than their "dense" counterparts. In addition to the structure of the resulting hydration product, such behaviour is extremely triggered by the pore size distribution and the specific surface area of the foam and by the lack of filler [38]. If blended GPs are produced, the amount, width and size of shrinkage-induced cracks can be reduced. The partial replacement of MK by ground-granulated blast furnace slag (GGBFS) is generally considered to have a beneficial effect on the mechanical properties of geopolymers. This observation is true for non-foamed GPs, especially when they are mixed with some aggregate (e.g., sand). Samson et al. [36] prepared aggregate-free blended MK-GGBFS geopolymers that were free of cracks. They found that the degree of shrinkage could be reduced, and the strength values could increase as long as the slag content did not exceed the amount of MK. In this case, slag particles were able to reduce the strong shrinkage caused by weight loss by way of acting as a solid aggregate. It is important to note that the authors only discussed the shrinkage/cracking properties of bulk (non-foamed) GPs; no such data were reported for foams. Although there are some sources that have reported the cracking tendency of blended bulk geopolymers, to the best of our knowledge, there is none of the relevant literature that deals with the shrinkage/cracking behaviour of blended MK-GGBFS GP foams.

So that cracks could be avoided, MK was partially replaced by GGBFS (10–50 wt%) in this study. For ensuring identical experimental conditions, the samples were mixed, heat-treated and stored as described in the section "Sample Preparation" (Section 2.2). Contrary to the literature, it was found that the shrinkage and crack tendency of the foams—even at the lowest slag content (10 wt%)—increased (Figure 9), and the strength values decreased accordingly ($\sigma_{compressive} \leq 1$ MPa). A further increase in the amount of GGBFS had a negative effect on the mechanical stability; the foams even fell into pieces, in some cases. The negative effects of slag addition can be caused by several factors. The geopolymerisation processes take place faster in the case of GGBFS, because slag has a high calcium content and, thus, has a higher pozzolanic reactivity than MK. However, the faster reaction results in the formation of a microstructure with a high pore content and thin cell walls. This weak microstructure cannot provide sufficient strength to handle the stresses resulting from volume change caused by shrinkage, which leads to cracking of the structure. Shrinkage at high "rates" is also facilitated by the fact that the water content—

required for incorporation but quasi-excessive for geopolymerisation—can escape faster from the connected pore structure formed during foaming. For this reason, the process of the above-mentioned volume change leads to more intense cracking of the foams.



(**a**) (**b**) (**c**)

Figure 9. Effect of slag addition ((**a**) 10, (**b**) 30 and (**c**) 50 wt%) on the shrinkage of foams.

Even if the porosity of the samples increased (P_{open}: 40–50 vol%) and there was no significant change in their thermal conductivity (Table 5), under the conditions used in this study, the production of MK-GGBFS blended foams cannot be recommended due to their poor mechanical stability. However, it should be noted that the addition of slag created an advantage. Along with an increase in the GGBFS content, the foams showed a more homogeneous pore size distribution, while, in the case of the 10 wt% GGBFS content, the pore diameter was in the range of 100–400 µm; up to 50 wt% GGBFS content, it was in the range of 250–400 µm.

Table 5. Effect of slag addition on the physical properties of foams.

GGBFS Content (wt%)	Compressive Strength (MPa)	Open Porosity (vol%)	Heat Conductivity (W/mK)
0	2.2 ± 0.2	36.9 ± 0.3	0.052 ± 0.002
10	1.0 ± 0.1	37.5 ± 0.4	0.052 ± 0.003
20	1.0 ± 0.2	38.1 ± 0.4	0.052 ± 0.005
30	0.9 ± 0.1	45.0 ± 0.6	0.053 ± 0.002
40	0.8 ± 0.3	51.9 ± 0.8	0.055 ± 0.003
50	0.5 ± 0.1	49.1 ± 1.2	0.052 ± 0.001

3.3.4. Changes in the Storage and Heat Treatment Parameters

During storage, several hairline cracks appeared on the surfaces of the samples, which could be caused by a dehydration process taking place via the surface [39,40]. For the production of crack-free specimens, it is essential to ensure an adequate water content, as the quantity of water can affect the speed of the bonding and solidification processes (dissolution, hydrolysis and polycondensation) in each stage and will consequently impact the properties of the final product. So that an abrupt loss of free water could be avoided, the samples were stored under water (T = 21–23 °C) after demoulding. Although the degree of cracking appeared to be reduced, cracking could not be eliminated completely, and the samples' compressive strengths and apparent porosities also deteriorated (Table 6).

Table 6. Effect of the storage conditions on the physical properties of foams.

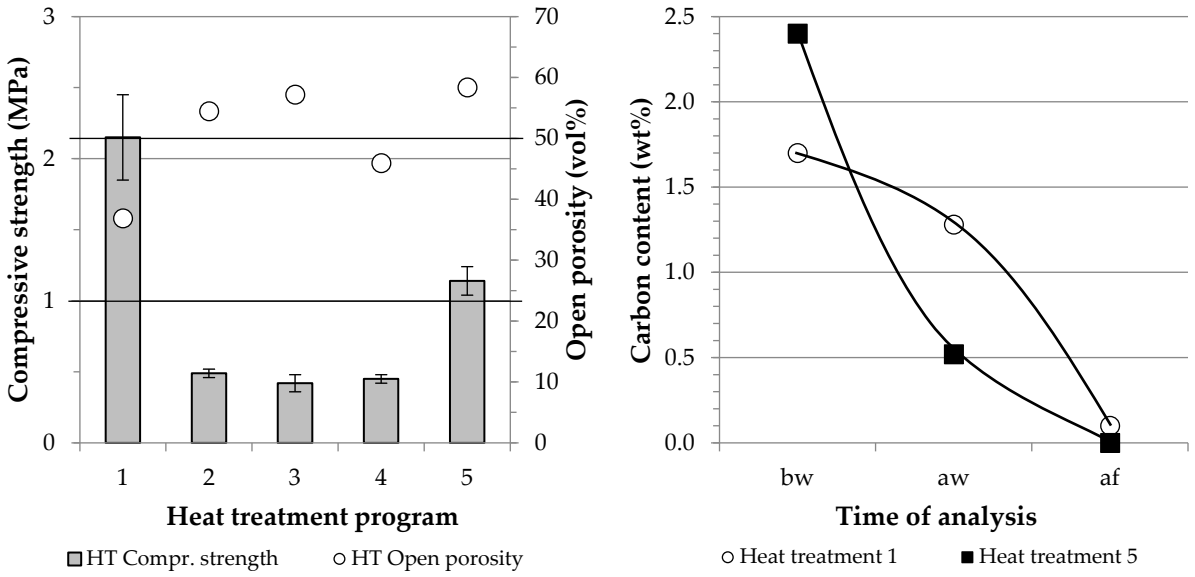
Storage Conditions	Compressive Strength (MPa)	Open Porosity (vol%)	Heat Conductivity (W/mK)
T_r atm	2.2 ± 0.2	36.9 ± 0.3	0.052 ± 0.002
T_r water	2.0 ± 0.1	31.3 ± 0.5	- *

T_r atm: curing under ambient conditions (21–23 °C and 50 ± 10% RH) until testing after demoulding, and T_r water: storage at 20 ± 2 °C under water until testing after demoulding. * In the case of underwater storage, the thermal conductivity of the specimen measured in a water-saturated state does not provide relevant information.

In order to produce crack-free foams, the rapid removal of moisture as a result of heat treatment should be avoided during the bonding mechanism of the samples. This can be achieved by altering the initial heat treatment parameters. Originally, after mixing, the slurry was heat-treated at ambient conditions for 24 h and at 75 °C for another 24 h in a sealed mould. Theoretically, the first step of the heat treatment is necessary for preventing cracking caused by the abrupt loss of water and for facilitating the geopolymerisation reaction, whereas the second step supports the solidification mechanism [30]. As a consequence, this mode of heat treatment can lead to an increase in the rate of geopolymerisation and an improvement in the compressive strength. However, surface hairline cracks and internal microcracks can be observed in the foams after heat treatment. Therefore, afterwards, by way of increasing the temperature of the heat treatment in the initial stage of the geopolymerisation, bonding and solidification reactions were facilitated, as this can also shorten the duration of the heat treatment. An increase in the temperature can also promote a saponification reaction by enhancing the formation of the surfactant that is responsible for foam stability. In addition, the effect of sealing the sample mould with plastic film (sealed sample mould: SM) and leaving it open (open sample mould: OM) was also investigated with respect to the crack tendency. Following a review of the relevant literature [16,25,29,30,32], it can be stated that there is no uniformly accepted heat treatment method for GP foams produced by the SPG combined route. The studies agree that, in the initial stage of the bonding and solidification processes, it is preferable to use a sealed sample mould to retain the moisture required for hydrolysis. Later, however, it is recommended to remove the plastic film so that excess water will evaporate and will not kinetically inhibit the polycondensation reaction. In light of this, in addition to the original heat treatment method, four additional programmes were selected:

1. 24 h at 21–23 °C and another 24 h at 75 °C in SM (original heat treatment conditions),
2. 24 h at 40 °C in SM,
3. 24 h at 60 °C in SM,
4. 24 h at 60 °C in OM,
5. 1 h at 80 °C in SM and another 4 h at 80 °C in OM.

It is important to note that a shorter heat treatment time was chosen for the last heat treatment mode, because a long heat treatment time (24 h) at this temperature would decrease the strength values [25]. Additionally, it must be remembered that an increase in the temperature results in greater reactivity and faster binding, which causes most of the bubbles to be trapped in the matrix in the initial stages of their formation, thereby increasing the porosity of the samples. This, however, reduces the compressive strength of the foams. Figure 10a shows the obtained compressive strength and open porosity values.



(**a**) (**b**)

Figure 10. Effect of heat treatment conditions on (**a**) the compressive strength and apparent porosity and (**b**) organic carbon content (Horizontal lines indicate boundary conditions in the case of the experimental job).

The first four heat treatment methods led to cracking of the samples, but the last method (No. 5) could produce crack-free specimens that met both the strength and porosity requirements and had extremely good thermal insulation properties: $\sigma_{compressive}$ = 1.1 MPa, P_{open} = 58.4 vol% and λ = 0.044 W/mK. In addition, the organic matter content of these samples was reduced through washing more than in the case of the original heat treatment method No. 1 (Figure 10b), and the organic matter content was completely removed through firing. This shorter heat treatment at elevated temperatures (1 h/80 °C in SM and then 4 h/80 °C in OM) not only accelerated the geopolymerisation reaction and catalysed the decomposition of H_2O_2 but also promoted the saponification process. This ultimately resulted in an increase in the amount of interconnected and open pores (Figure 11). The pore diameter of the foams was in the range of 100–300 µm (average pore diameter: 184 ± 45 µm).

Based on the results, it can be stated that the method developed in the scope of this study can be used to produce geopolymer foam-based products that approximate the strength of the building materials and can practically be considered a thermal insulation material (thermal conductivity must be lower than 0.065 W/mK, according to the ISO and CEN standards). A material with similar appearance and of similar properties is, for example, glass foam. However, the production of glass foams is not only significantly more expensive, but the thermal conductivity of a slab with a compressive strength of 1.0 MPa also exceeds 0.1 W/mK [41,42].

The firing of GP foams was used to remove the organic matter content, on the one hand, and it also further improved the results achieved so far, on the other hand. During the heat treatment at 600 °C, the condensation/polymerisation of the Si/Al-OH groups triggered an increase in the strength values, whereas the removal of water and glycerol molecules from the pores increased the open porosity of the samples and improved their thermal insulation. The development of the physical properties is shown in Figure 12.

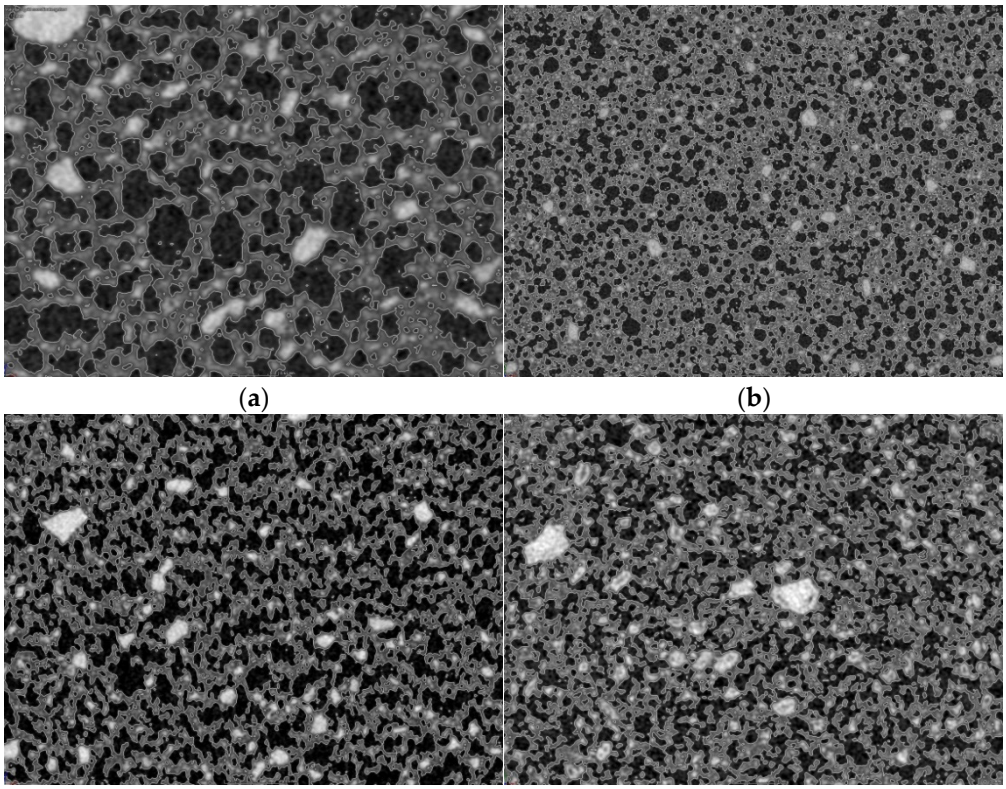


Figure 11. Effect of foaming components and heat treatment conditions on the pore structure of (**a**) S-4.5, (**b**) S-4.5-0.1, (**c**) S-4.5-0.1 treated with method No. 5 and (**d**) S-4.5-0.1 treated with method No. 5 after firing.

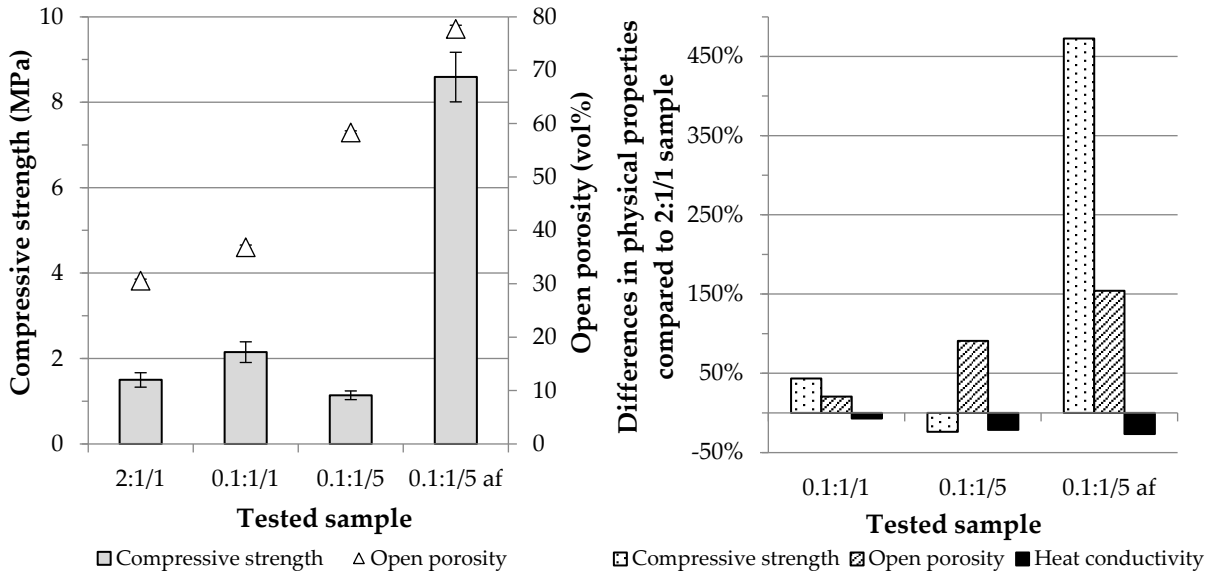


Figure 12. Comparison of the optimal results in the case of each experimental phase: (**a**) effect of experimental parameters on compressive strength and open porosity and (**b**) differences in physical properties compared to 2:1/1 sample (Samples designated as the "stabilising agent:peroxid ratio/number of heat treatment method").

Based on the results, it can be concluded that the following significantly improved the physical properties: a reduction to 1/20 of the original amount of sunflower oil used as the stabilising agent (from 2.0:1.0 to 0.1:1.0 S:F ratio), changes in the heat treatment conditions (24 h/21–23 °C + 24 h/75 °C in SM → 1 h/80 °C in SM + 4 h/80 °C in OM) and firing the samples. Through the use of the parameters described in the present study, high-strength (8.6 MPa) and high open porosity (77.7 vol%) foamed geopolymers can be developed. In addition, due to their low bulk density, thermal conductivity (0.041 W/mK) and high specific surface area (Table 7), such foams will meet most of the requirements set out for thermal insulation materials and catalyst supports.

Table 7. Physical properties of developed GP foams for multifunctional applications.

Compressive Strength (MPa)	Open Porosity (vol%)	Heat Conductivity (W/mK)	Bulk Density (kg/m^3)	BET Surface Area (m^2/g)
8.6 ± 0.6	77.7 ± 0.7	0.041 ± 0.001	499 ± 17	4.3 ± 0.3

4. Conclusions

This paper aimed to produce and investigate metakaolin-based foams, of which the foaming process was carried out using a combined SPG process. The primary goal of the study was to find the optimal experimental parameters that can be used to develop multifunctional GP foams with controlled properties. Based on the experiments performed, the following conclusions can be drawn.

- Using a diluted H_2O_2 solution and varying the stabilising agent:peroxide (S:F) ratio, geopolymer foams with a designed porosity (5.8–67.5 vol%) and pore size distribution can be produced.
- From the point of view of these materials' practical applications (thermal insulation material and catalyst support), it is important to ensure an optimal strength–porosity relationship, which can be achieved through using sunflower oil, 4.5 wt% H_2O_2 solution and a 0.1:1.0 S:F ratio ($\sigma_{compressive}$ = 2.2 MPa, P_{open} = 36.9 vol%).
- The porosity and thermal insulation properties of the samples can be improved through a short-period heat treatment of 80 °C. The developed GP foams can practically be considered a thermal insulation material (λ = 0.044 W/mK), which has adequate compressive strength (1.1 MPa) and open porosity (58.4 vol%).
- A manufacturing process was developed that allows the production of multifunctional foams.
- A non-flammable, easy-to-cut, rodent-resistant thermal insulation material was produced that can act as a suitable alternative to glass foam.
- The organic matter contents of the samples can be removed through washing in the intermittent operation and then firing. The developed foams can also be used as catalyst supports in places subject to high mechanical stress (e.g., flowing liquid sewage) due to their adequate strength and high porosity.
- The final heat treatment at 600 °C enables the production of high-strength (8.6 MPa), open porosity (77.7 vol%) and low thermal conductivity (0.041 W/mK) products with remarkable potential for use in the scope of the above-mentioned higher value-added applications.

Author Contributions: Conceptualisation, A.B. and T.K.; methodology, A.B. and T.K.; software, A.B.; validation, A.B. and T.K.; investigation, A.B.; data curation, A.B.; writing—original draft preparation, A.B.; writing—review and editing, A.B. and T.K.; visualisation, A.B.; supervision, T.K. and funding acquisition, T.K. All authors have read and agreed to the published version of the manuscript.

Funding: This work has been implemented by the TKP2020-NKA-10 project with the support provided by the Ministry for Innovation and Technology of Hungary from the National Research, Development and Innovation Fund, financed under the 2020 Thematic Excellence Programme funding scheme.

Institutional Review Board Statement: Not applicable.

Informed Consent Statement: Not applicable.

Data Availability Statement: The data are contained within the article.

Acknowledgments: The SEM studies were performed at the electron microscopy laboratory of the University of Pannonia, established using grant no. GINOP-2.3.3-15-2016-0009 from the European Structural and Investments Funds and the Hungarian Government.

Conflicts of Interest: The authors declare no conflict of interest.

Appendix A

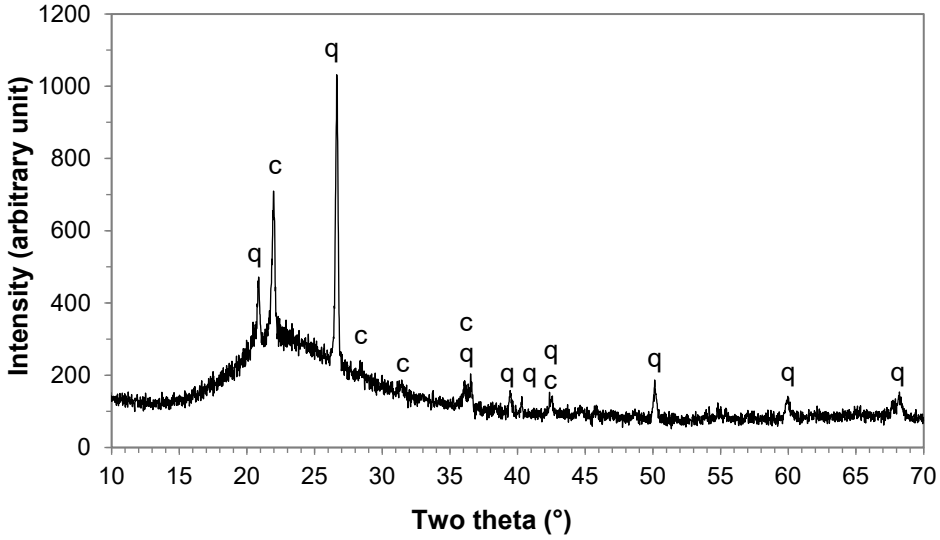


Figure A1. XRD pattern of MK (q: quartz PDF 33-1161 and c: cristobalite PDF 39-1425).

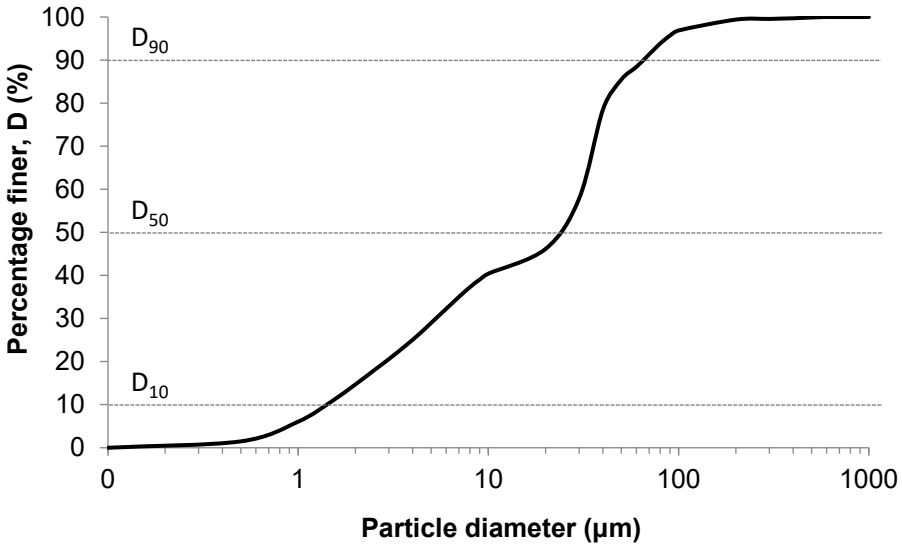


Figure A2. Particle size distribution of MK.

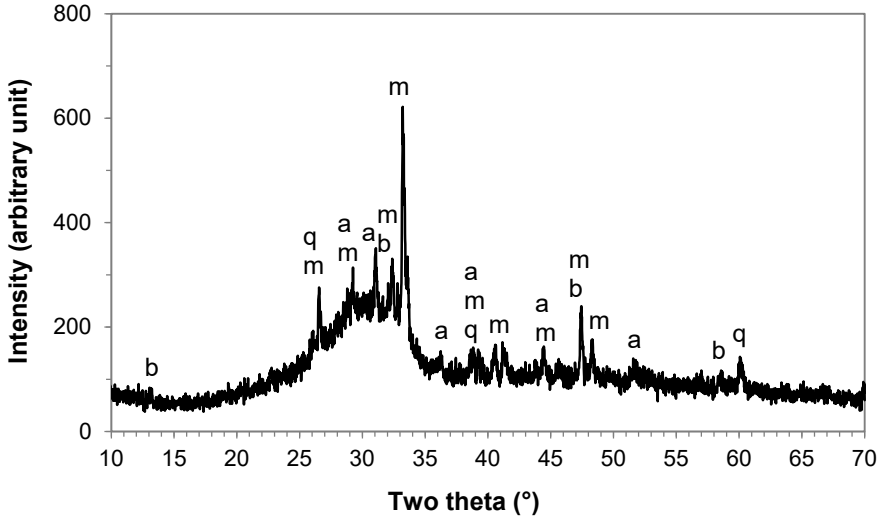


Figure A3. XRD pattern of GGBFS (m: merwinite PDF 35-0591, a: akermanite PDF 01-087-0046, b: brownmillerite PDF 01-074-3673 and q: quartz PDF 33-1161).

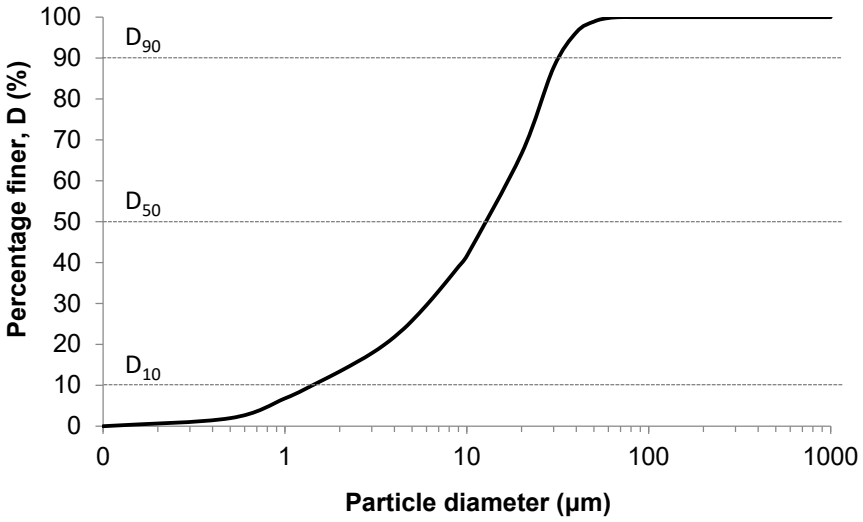


Figure A4. Particle size distribution of GGBFS.

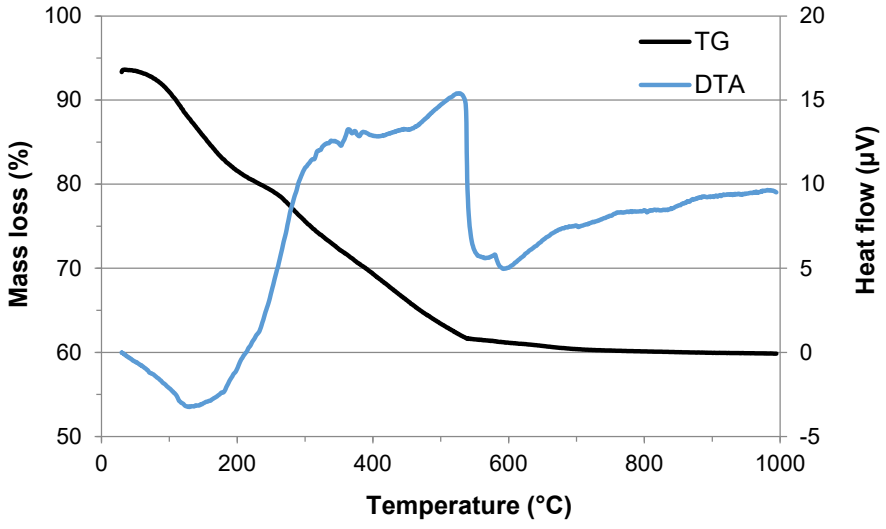


Figure A5. TG and DTA curves of sample S-4.5.

References

1. Davidovits, J. Geopolymers: Inorganic polymers new materials. *J. Therm. Anal.* **1991**, *37*, 1633–1656. [CrossRef]
2. Smith, J.W.; Comrie, D.C. Geopolymeric building materials in third world countries. In Proceedings of the 1st International Conference on Geopolymer '88, Compiegne, France, 1–3 June 1988.
3. Panias, D.; Giannopoulou, I.P.; Perraki, T. Effect of synthesis parameters on the mechanical properties of fly ash-based geopolymers. *Colloids Surf. A* **2007**, *301*, 246–254. [CrossRef]
4. Davidovits, J. Properties of geopolymer cements. In Proceedings of the First International Conference on Alkaline Cements and Concretes, Kiev, Ukraine, 11–14 October 1994.
5. Zhang, L. Production of bricks from waste materials—A review. *Constr. Build. Mater.* **2013**, *47*, 643–655. [CrossRef]
6. Ibrahim, W.M.W.; Hussin, K.; Abdullah, M.M.A.B.; Kadir, A.A.; Binhussain, M.A. Review of Fly Ash-Based Geopolymer Lightweight Bricks. *Appl. Mech. Mater.* **2015**, *754–755*, 452–456. [CrossRef]
7. El-Naggar, K.A.M.; Amin, S.K.; El-Sherbiny, S.A.; Abadir, M.F. Preparation of geopolymer insulating bricks from waste raw materials. *Constr. Build. Mater.* **2019**, *222*, 699–705. [CrossRef]
8. Jitsangiam, P.; Suwan, T.; Pimraksa, K.; Sukontasukkul, P.; Chindaprasirt, P. Challenge of adopting relatively low strength and self-cured geopolymer for road construction application: A review and primary laboratory study. *Int. J. Pavement Eng.* **2019**, *22*, 1454–1468. [CrossRef]
9. Cheng, T.W.; Chiu, J.P. Fire-resistant geopolymer produced by granulated blast furnace slag. *Miner. Eng.* **2003**, *16*, 205–210. [CrossRef]
10. Tan, Q.; Li, N.; Xu, Z.; Chen, X.; Peng, X.; Shuai, Q.; Yao, Z. Comparative performance of cement and metakaolin based-geopolymer blocks for strontium immobilization. *J. Ceram. Soc. Jpn.* **2019**, *127*, 44–49. [CrossRef]
11. Yunsheng, Z.; Wei, S.; Qianli, C.; Lin, C. Synthesis and heavy metal immobilization behaviors of slag based geopolymer. *J. Hazard. Mater.* **2007**, *143*, 206–213. [CrossRef]
12. Novais, R.M.; Pullar, R.C.; Labrincha, J.A. Geopolymer foams: An overview of recent advantages. *Prog. Mater. Sci.* **2020**, *109*, 100621. [CrossRef]
13. Alzeer, M.I.M.; MacKenzie, K.J.D.; Keyzers, R.A. Porous aluminosilicate inorganic polymers (geopolymers): A new class of environmentally benign heterogeneous solid acid catalysts. *Appl. Catal. A* **2016**, *524*, 173–181. [CrossRef]
14. Luukkonen, T.; Heponiemi, A.; Runtti, H.; Pesonen, J.; Yliniemi, J.; Lassi, U. Application of alkali-activated materials for water and wastewater treatment: A review. *Rev. Environ. Sci. Biotechnol.* **2019**, *18*, 271–297. [CrossRef]
15. Landi, E.; Medri, V.; Papa, E.; Dedecek, J.; Klein, P.; Benito, P.; Vaccari, A. Alkali-bonded ceramics with hierarchical tailored porosity. *Appl. Clay Sci.* **2013**, *73*, 56–64. [CrossRef]
16. Bai, C.; Colombo, P. Processing, properties and applications of highly porous geopolymers: A review. *Ceram. Int.* **2018**, *44*, 16103–16118. [CrossRef]
17. Papa, E.; Medri, V.; Kpogbemabou, D.; Morinière, V.; Laumonier, J.; Vaccari, A.; Rossignol, S. Porosity and insulating properties of silica-fume based foams. *Energy Build.* **2016**, *131*, 223–232. [CrossRef]
18. Hajimohammadi, A.; Ngo, T.; Mendis, P.; Sanjayan, J. Regulating the chemical foaming reaction to control the porosity of geopolymer foams. *Mater. Des.* **2017**, *120*, 255–265. [CrossRef]
19. Kamseu, E.; Nait-Ali, B.; Bignozzi, M.C.; Leonelli, C.; Rossignol, S.; Smith, D.S. Bulk composition and microstructure dependence of effective thermal conductivity of porous inorganic polymer cements. *J. Eur. Ceram. Soc.* **2012**, *32*, 1593–1603. [CrossRef]
20. Leiva, C.; Luna-Galiano, Y.; Arenas, C.; Alonso-Fariñas, B.; Fernández-Pereira, C. A porous geopolymer based on aluminum-waste with acoustic properties. *Waste Manag.* **2019**, *95*, 504–512. [CrossRef]
21. Feng, J.; Zhang, R.; Gong, L.; Li, Y.; Cao, W.; Cheng, X. Development of porous fly ash based geopolymer with low thermal conductivity. *Mater. Des.* **2015**, *65*, 529–533. [CrossRef]
22. Novais, R.M.; Buruberri, L.H.; Ascensão, G.; Seabra, M.P.; Labrincha, J.A. Porous biomass fly ash geopolymers with tailored thermal conductivity. *J. Clean. Prod.* **2016**, *119*, 99–107. [CrossRef]
23. Palmero, P.; Formia, A.; Antonaci, P.; Brini, S.; Tulliani, J.M. Geopolymer technology for application-oriented dense and lightened materials. Elaboration and characterization. *Ceram. Int.* **2015**, *41*, 12967–12979. [CrossRef]
24. Masi, G.; Rickard, W.D.A.; Vickers, L.; Bignozzi, M.C.; van Riessen, A. A comparison between different foaming methods for the synthesis of light weight geopolymers. *Ceram. Int.* **2014**, *40*, 13891–13902. [CrossRef]
25. Verdolotti, L.; Liguori, B.; Capasso, I.; Ericco, A.; Caputo, D.; Lavorgna, M.; Iannace, S. Synergistic effect of vegetable protein and silicon addition on geopolymeric foams properties. *J. Mater. Sci.* **2015**, *50*, 2459–2466. [CrossRef]
26. Cilla, M.S.; Colombo, P.; Morelli, M.R. Geopolymer foams by gelcasting. *Ceram. Int.* **2014**, *40*, 5723–5730. [CrossRef]
27. Petlitckaia, S.; Poulesquen, A. Design of lightweight metakaolin based geopolymer foamed with hydrogen peroxide. *Ceram. Int.* **2019**, *45*, 1322–1330. [CrossRef]
28. Traven, K.; Češnovar, M.; Škapin, S.D.; Ducman, V. High temperature resistant fly ash and metakaolin-based alkali-activated foams. *Ceram. Int.* **2021**, *47*, 25105–25120. [CrossRef]
29. Cilla, M.S.; de Mello Innocentini, M.D.; Morelli, M.R.; Colombo, P. Geopolymer foams obtained by the saponification/peroxide/gelcasting combined route using different soap foam precursors. *J. Am. Ceram. Soc.* **2017**, *100*, 3440–3450. [CrossRef]

30. Bai, C.; Franchin, G.; Elsayed, H.; Conte, A.; Colombo, P. High strength metakaolin-based geopolymer foams with variable macroporous structure. *J. Eur. Ceram. Soc.* **2016**, *36*, 4243–4249. [CrossRef]
31. Bai, C.; Colombo, P. High-porosity geopolymer membrane supports by peroxide route with the addition of egg white as surfactant. *Ceram. Int.* **2017**, *43*, 2267–2273. [CrossRef]
32. Bai, C.; Ni, T.; Wang, Q.; Li, H.; Colombo, P. Porosity, mechanical and insulating properties of geopolymer foams using vegetable oil as the stabilizing agent. *J. Eur. Ceram. Soc.* **2018**, *38*, 799–805. [CrossRef]
33. Asim, N.; Alghoul, M.; Mohammad, M.; Amin, M.H.; Akhtaruzzaman, M.; Amin, N.; Sopian, K. Emerging sustainable solutions for depollution: Geopolymers. *Constr. Build. Mater.* **2019**, *199*, 540–548. [CrossRef]
34. Sazama, P.; Bortnovsky, O.; Ďedeček, J.; Tvarůžková, Z.; Sobalík, Z. Geopolymer based catalysts—New group of catalytic materials. *Catal. Today* **2011**, *164*, 92–99. [CrossRef]
35. Macphee, D.E.; Folli, A. Photocatalytic concretes—The interface between photocatalysis and cement chemistry. *Cem. Concr. Res.* **2016**, *85*, 48–54. [CrossRef]
36. Samson, G.; Cyr, M.; Gao, X.X. Thermomechanical performance of blended metakaolin-GGBS alkali-activated foam concrete. *Constr. Build. Mater.* **2017**, *157*, 982–993. [CrossRef]
37. Wang, Z.; Lu, D. Study on the effect of emulsifiers on the pore structures of geopolymer prepared by emulsing templating. *Mater. Res. Express* **2020**, *7*, 055508. [CrossRef]
38. Zhang, G.; Provis, J.L.; Reid, A.; Wang, H. Geopolymer foam concrete: An merging material for sustainable construction. *Constr. Build. Mater.* **2014**, *56*, 113–127. [CrossRef]
39. Zuhua, Z.; Xiao, Y.; Huajun, Z.; Yue, C. Role of water in the synthesis of calcined kaolin-based geopolymer. *Appl. Clay Sci.* **2009**, *43*, 218–223. [CrossRef]
40. Kuenzel, C.; Vandeperre, L.J.; Donatello, S.; Boccaccini, A.R.; Cheeseman, C. Ambient temperature drying shrinkage and cracking in metakaolin-based geopolymers. *J. Am. Ceram. Soc.* **2012**, *95*, 3270–3277. [CrossRef]
41. Stochero, N.P.; de Souza Chami, J.O.R.; Souza, M.T.; de Moraes, E.G.; de Oliveira, A.P.N. Green glass foams from wastes designed for thermal insulation. *Waste Biomass Valoriz.* **2021**, *12*, 1609–1620. [CrossRef]
42. Owoeye, S.S.; Matthew, G.O.; Ovienmhanda, F.O.; Tunmilayo, S.O. Preparation and characterization of foam glass from waste container glasses and water glass for application in thermal insulations. *Ceram. Int.* **2020**, *46*, 11770–11775. [CrossRef]